Cardiovascular Research (2013) **99**, 382–394
doi:10.1093/cvr/cvt106

Nuclear accumulation of androgen receptor in gender difference of dilated cardiomyopathy due to lamin A/C mutations

Takuro Arimura[1], Kenji Onoue[2,3,4], Yumiko Takahashi-Tanaka[1], Taisuke Ishikawa[1], Masayoshi Kuwahara[5], Mitsutoshi Setou[4,6,7], Shuji Shigenobu[8], Katsushi Yamaguchi[8], Anne T. Bertrand[9,10], Noboru Machida[11], Kazumi Takayama[11], Masayuki Fukusato[11], Ryo Tanaka[12], Satoshi Somekawa[2,3], Tomoya Nakano[2,3], Yoshihisa Yamane[12], Keiji Kuba[13], Yumiko Imai[13], Yoshihiko Saito[2,3], Gisèle Bonne[9,10,14], and Akinori Kimura[1]*

[1]Department of Molecular Pathogenesis, Medical Research Institute, Tokyo Medical and Dental University, 1-5-45 Bunkyo-Ku, Tokyo 113-8510, Japan; [2]First Department of Internal Medicine, Nara Medical University, Kashihara, Japan; [3]Department of Regulatory Medicine for Blood Pressure, Nara Medical University, Kashihara, Japan; [4]Department of Cell Biology and Anatomy, Hamamatsu University School of Medicine, Hamamatsu, Japan; [5]Department of Comparative Pathophysiology, Graduate School of Agriculture and Life Sciences, The University of Tokyo, Tokyo, Japan; [6]Systems Molecular Anatomy Laboratory, Medical Photonics Research Center, Hamamatsu University, School of Medicine, Hamamatsu, Japan; [7]National Institute for Physiological Sciences, Okazaki, Japan; [8]National Institute for Basic Biology, Okazaki, Japan; [9]INSERM, U974, Paris, France; [10]Université Pierre et Marie Curie-Paris 6, UM 76, CNRS, UMR 7215, Institut de Myologie, Paris, France; [11]Department of Veterinary Clinical Oncology, Faculty of Agriculture, Tokyo University of Agriculture and Technology, Tokyo, Japan; [12]Department of Veterinary Surgery, Faculty of Agriculture, Tokyo University of Agriculture and Technology, Tokyo, Japan; [13]Department of Biological Informatics and Experimental Therapeutics, Akita University Graduate School of Medicine, Japan; and [14]AP-HP, Groupe Hospitalier Pitié-Salpêtrière, U.F. Cardiogénétique et Myogénétique, Service de Biochimie Métabolique, Paris, France

Received 30 August 2012; revised 19 April 2013; accepted 24 April 2013; online publish-ahead-of-print 30 April 2013

Time for primary review: 27 days

Aims Dilated cardiomyopathy (DCM) is characterized by ventricular dilation associated with systolic dysfunction, which could be caused by mutations in lamina/C gene (*LMNA*). *LMNA*-linked DCM is severe in males in both human patients and a knock-in mouse model carrying a homozygous p.H222P mutation ($Lmna^{H222P/H222P}$). The aim of this study was to investigate the molecular mechanisms underlying the gender difference of *LMNA*-linked DCM.

Methods and results A whole-exome analysis of a multiplex family with DCM exhibiting the gender difference revealed a DCM-linked *LMNA* mutation, p.R225X. Immunohistochemical analyses of neonatal rat cardiomyocytes expressing mutant *LMNA* constructs and heart samples from the *LMNA*-linked DCM patients and $Lmna^{H222P/H222P}$ mice demonstrated a nuclear accumulation of androgen receptor (AR) and its co-activators, serum response factor, and four-and-a-half LIM protein-2. Role of sex hormones in the gender difference was investigated *in vivo* using the $Lmna^{H222P/H222P}$ mice, where male and female mice were castrated and ovariectomized, respectively, or treated with testosterone or an antagonist of AR. Examination of the mice by echocardiography, followed by the analyses of histological changes and gene/protein expression profiles in the hearts, confirmed the involvement of testicular hormone in the disease progression and enhanced cardiac remodelling in the $Lmna^{H222P/H222P}$ mice.

Conclusion These observations indicated that nuclear accumulation of AR was associated with the gender difference in *LMNA*-linked DCM.

Keywords Dilated cardiomyopathy • Gender difference • Androgen receptor • Testosterone • Lamin A/C

1. Introduction

Dilated cardiomyopathy (DCM), a primary cardiac muscle disorder characterized by ventricular chamber dilation and systolic dysfunction,[1] is the major cause of chronic heart failure (CHF) and the most common indication for cardiac transplantation.[2] Underlying aetiologies include genetic, viral, toxic agents like alcohol, mitochondrial, and metabolic disorders.[2] It is known that familial occurrence is seen in ~30–40% of

* Corresponding author. Tel: +81 3 5803 4905; fax: +81 3 5803 4907, Email: akitis@mri.tmd.ac.jp

DCM patients.[3] To date, mutations in more than 30 genes encoding components of sarcomere, sarcolemma, cytoskeletons, or nuclear envelope have been discovered in patients with DCM,[4] and 8% of familial and sporadic DCM may be caused by mutations in *LMNA* encoding lamin A/C.[5]

DCM occurs more frequently in men than in women (male to female ratio: 2.5),[6] and a recent study revealed significant gender differences in cardiac phenotypes such as a higher mortality and severer cardiac dysfunction in male DCM patients carrying *LMNA* mutation.[7] It has been suggested that gonadal hormones, such as testosterone and oestrogens, may explain the gender difference in cardiac phenotypes. Results from *in vitro* and *in vivo* studies suggest that oestrogen may play a pivotal role,[8,9] in part due to protective actions of female hormones, which was evidenced by increased cardiovascular risk in women after menopause and by cardiovascular benefits of oestrogen replacement therapy.[9] However, mechanisms for the gender difference in DCM remain unknown.

We have established a 'knock-in' mouse carrying a p.H222P mutation of *Lmna*.[10] Homozygous knock-in mice (*Lmna*$^{H222P/H222P}$) developed DCM phenotypes, including progressive left ventricular (LV) dilation and contractile dysfunction from 2 and 4 months of age in males and females, respectively.[10] *Lmna*$^{H222P/H222P}$ male mice displayed more prominent abnormalities in cardiac function than females, and they died of CHF between 4 and 10 months of age, while female mice died at 6 and 13 months of age,[10] indicating that the *Lmna*$^{H222P/H222P}$ mice are a good model for studying the gender difference in the *LMNA*-linked DCM. On the other hand, no gender difference was observed in another knock-in mouse model with a *LMNA* mutation, p.delK32,[11] suggesting that not all of *LMNA* mutations were associated with the gender difference.

In this study, we first identified a *LMNA* mutation, p.R225X, in a DCM family in which apparent gender difference in clinical course of DCM was observed. Transfection experiments of neonatal rat cardiomyocytes (NRCs) with the normal or mutant *LMNA* construct revealed that the p.R225X and p.H222P mutations induced nuclear accumulation of endogenous androgen receptors (AR), while such phenomena were not found with normal or p.delK32 mutation. The nuclear accumulation of AR was accompanied by testosterone-induced nuclear translocation of four-and-a-half LIM protein-2 (FHL2) and serum response factor (SRF), which were involved in the cardiac remodelling process. *In vivo* studies revealed the adverse effect of testosterone in the cardiac function and pathological changes in the heart of *Lmna*$^{H222P/H222P}$ mice. We report here the involvement of AR and testosterone as a molecular basis for the gender difference in the progression of DCM caused by specific *LMNA* mutations.

2. Methods

Experimental details including methods of anaesthesia are described in Supplementary Information.

2.1 Mutational analysis

All human subjects and tissues were collected in accordance with the principles outlined in the Declaration of Helsinki. Whole-exome and sequencing analyses were performed with genomic DNA samples obtained from the subjects after given informed consent. The protocol for research was approved by the Ethics Reviewing Committees of Medical Research Institute, Tokyo Medical and Dental University, and Nara Medical University.

2.2 Heart tissues

Paraffin-embedded LV myocardial tissues obtained at autopsy from three male patients with DCM carrying the p.R225X mutation, from two male patients with DCM carrying no *LMNA* mutation, and from two control subjects without DCM were analysed. Informed consent was given from relatives of each subject. Heart samples from the *Lmna*$^{H222P/H222P}$ [10] ($n = 4$), guanylyl cyclase A knock out (GC-A KO)[12] ($n = 3$), and transverse aortic constriction (TAC)[13] ($n = 2$) mice were prepared, as described previously.[10]

2.3 Immunofluorescence microscopy

All tissue sections and cells were prepared for immunofluorescence microscopy and analysed as described previously.[14,15]

2.4 Animals

Establishment of *Lmna*$^{H222P/H222P}$ mouse line was reported previously.[10] Mice were fed with a chow diet and housed in a barrier facility. All care and experimental procedures of animals were in accordance with the guidelines for the Care and Use of Laboratory Animals published by the National Institute of Health (NIH Publication, eighth edition, 2011) and subjected to prior approval by the local animal protection authority in Tokyo Medical and Dental University.

2.5 Castration and ovariectomy

Six-week-old male and female wild-type (WT, *Lmna*$^{+/+}$) and *Lmna*$^{H222P/H222P}$ mice before puberty underwent bilateral castration and ovariectomy, respectively, under anaesthesia.

2.6 Treatment with testosterone or flutamide

Castrated male mice ($n = 16$ and 20 of WT and *Lmna*$^{H222P/H222P}$ mice, respectively) and non-operated female mice ($n = 16$ and 21 of WT and *Lmna*$^{H222P/H222P}$ mice, respectively) were subcutaneously implanted with a 25 mm long silascon tube (inner diameter, 2.0 mm; outer diameter, 3.0 mm; Kaneka medix) containing crystalline testosterone under anaesthesia.[16] Non-operated male mice ($n = 16$ and 20 of WT and *Lmna*$^{H222P/H222P}$ mice, respectively) were also implanted subcutaneously with the tube containing crystalline flutamide, an AR antagonist (Sigma-Aldrich). Empty tubes were implanted in sham-operated animals (males: $n = 16$ and 19 of WT and *Lmna*$^{H222P/H222P}$ mice; females: $n = 16$ and 21 of WT and *Lmna*$^{H222P/H222P}$ mice, respectively). Testosterone- or flutamide-containing tubes were incubated in the saline at 37° for 24 h before implantation to avoid a surge-like release after implantation. The implanted tubes were not removed throughout the experiments.

2.7 Echocardiography, electrocardiography (ECG), and blood pressure measurement

Transthoracic echocardiography, electrocardiography (ECG) analysis, and measurement of systolic blood pressure and heart rate were performed, as described previously.[17,18]

2.8 Histopathological examinations

Histopathological examination using haematoxylin–eosin or Masson's trichrome staining was done by the standard methods ($n = 4$, each group). Measurement of interstitial fibrosis area and quantitative analysis of collagen in the heart were performed ($n = 6$, each group), as described previously.[18]

2.9 Ribonucleic acid (RNA) isolation and quantitative expression analysis

Total RNA extraction, complementary deoxyribonucleic acid (cDNA) synthesis, and real-time reverse transcription (RT)–polymerase chain reaction (PCR) analysis were performed ($n = 6$ in each group) as described previously.[18] Relative steady-state levels of messenger RNA (mRNA)

were calculated using a comparative Ct (ΔδCT) method.[19] Individual expression values were normalized against the level of *Gapdh* mRNA.

2.10 Protein extraction and immunoblotting

Total cellular protein was extracted ($n = 4$, each group) as described previously.[15] Nuclear protein fraction was prepared ($n = 8$, each group) using NE-PER Nuclear and Cytoplasmic Extraction Regents (Pierce). Western blotting analysis was performed using primary antibodies against β-myosin heavy chain (βMHC), atrial natriuretic peptide (ANP), AR, SRF, FHL2, emerin, and glyceraldehyde 3-phosphate dehydrogenase (GAPDH) (Santa Cruz). The signal obtained for GAPDH was used as an internal control to normalize the amounts of protein on the immunoblots.

2.11 Measurement of serum testosterone level

Blood samples were obtained by heart puncture at time of necropsy and serum testosterone level was measured by radioimmunoassay using a DPC total testosterone kit (Mitsubishi chemical Medicine).

2.12 Statistical analysis

Phenotypic data were acquired by observers who were blinded to the genotype of mice. Numerical data were expressed as means ± SEM. Statistical differences were analysed using two-way analysis of variance (ANOVA) and then evaluated using a Tukey adjustment for the *post hoc* test. Survival curves were drawn for each group with the Kaplan–Meier method and the differences were compared by a log-rank test. A *P*-value <0.05 was considered to be statistically significant.

3. Results

3.1 Mutational analysis

We found a DCM family in which affected males had severer symptoms and phenotypes than females at the time of onset (*Figure 1* and see Supplementary material online, *Table S1*); all affected males had abnormalities both in cardiac conduction system and cardiac function at around the age of 30s to early 40s, whereas affected females had abnormalities in the cardiac conduction system at around the age of 40s and developed mild cardiac dysfunction later identified several sequence variations (see Supplementary material online, *Table S2*) including a *LMNA* mutation (c.673C>T, p.R225X) in the tested members, and a subsequent direct sequencing analysis revealed that all affected individuals and no unaffected members carried the p.R225X mutation, demonstrating a linkage of *LMNA* mutation to DCM with a LOD score of 3.01. This finding was consistent with that the *LMNA* mutations were associated with cardiac conduction disorder and gender difference in humans[7] and in *Lmna*$^{H222P/H222P}$.[10]

3.2 Accumulation of AR in nuclei of cardiomyocytes expressing LMNA with specific mutations

Because sexual hormones mediate their functions via specific receptor, we investigated whether the cellular localization of AR and estrogenic receptor (ER) α and β would be affected by specific *LMNA* mutations. We analysed NRCs transfected with Flag-tagged WT or mutant *LMNA* constructs carrying p.R225X, p.H222P, or p.delK32. Endogenous AR was found in both cytoplasm and nucleus in the cells expressing normal *LMNA* or *LMNA* with p.delK32, whereas increased nuclear accumulation of AR in the absence of androgen was observed in the most (~90%) of cells expressing *LMNA* with p.H222P or p.R225X (*Figure 2A*). In contrast, no apparent differences in the localization of ERα and ERβ were observed among the transfected NRCs (see Supplementary material online, *Figure S1*). On the other hand, nuclear accumulation of AR was not evident in HeLa cells transfected with the Flag-tagged WT or mutant LMNA constructs (see Supplementary material online, *Figure S2*). These observations implied that the cardiomyocyte-specific nuclear accumulation of AR was associated with specific *LMNA* mutations exhibiting the gender difference.

3.3 Nuclear accumulation of AR in the heart muscle

Because the findings in the transfection experiments might be due to the overexpression of *LMNA* with mutations, we next investigated whether the nuclear accumulation of AR could be found in the heart muscle carrying the *LMNA* mutations. AR was found mainly in the cytoplasm in heart samples from a control and a DCM patient without any *LMNA* mutations,

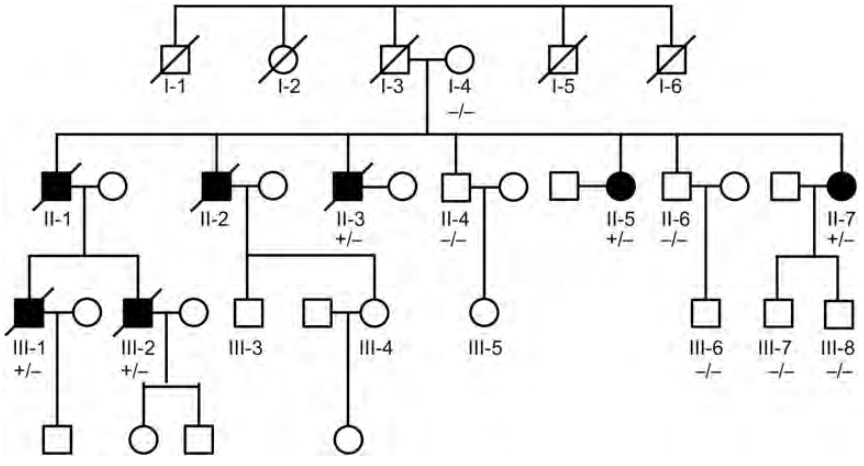

Figure 1 Pedigree tree of a DCM family Squares represent males; circles represent females. The presence (+/−) or absence (−/−) of the c.673C>T, p.R225X mutation in *LMNA* is indicated for the analysed subjects. Filled symbols indicate those with clinical symptoms and slashed indicate the deceased subjects.

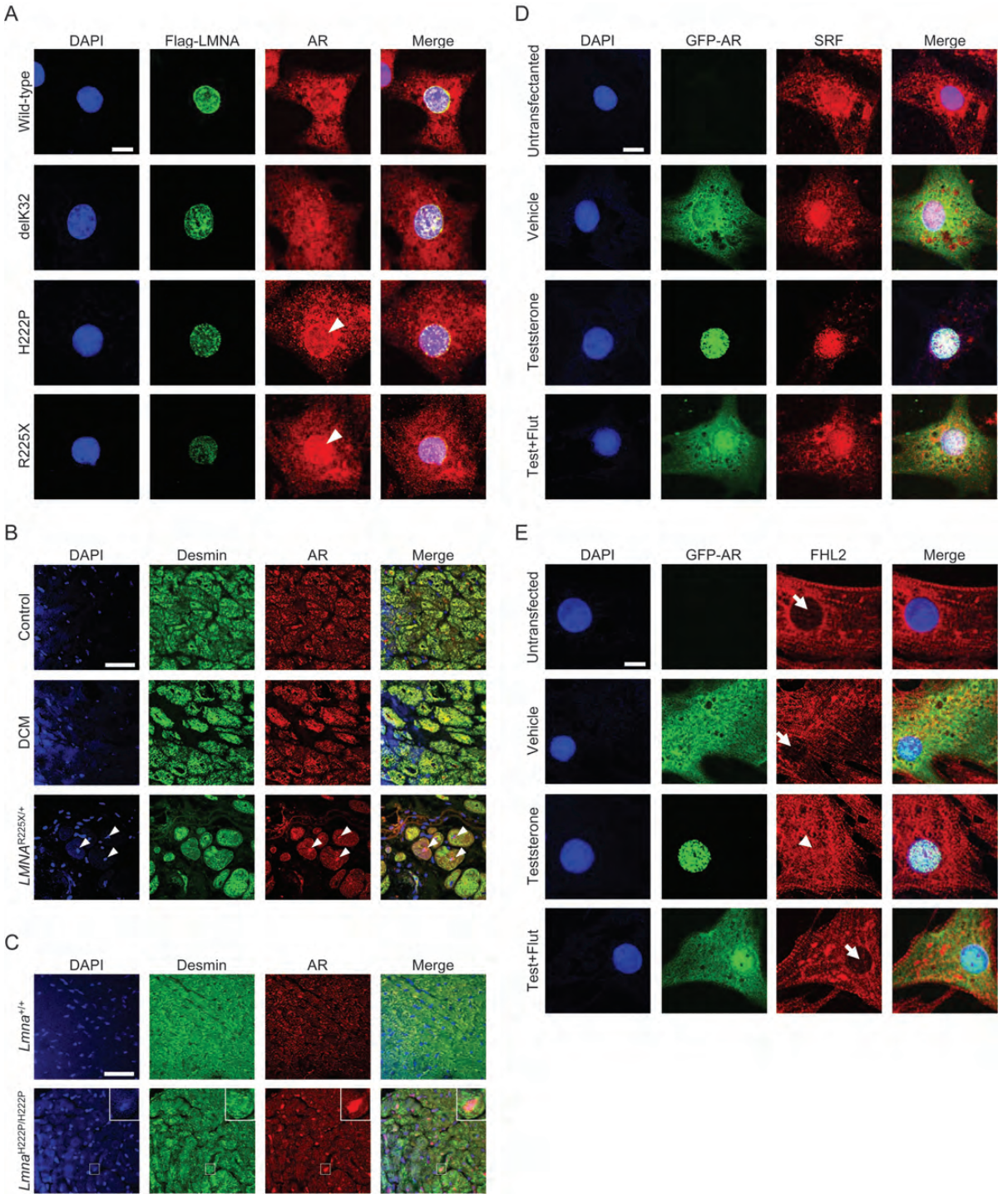

Figure 2 Localization of AR in cardiomyocytes. (*A*) NRCs transfected with Flag-tagged LMNA-WT, -p.delK32, -p.H222P, or -p.R225X construct were stained with DAPI, anti-Flag ,or anti-AR antibody. Merged images are also shown. Arrows indicate the accumulation of AR in nuclei; scale bars=10 μm. (*B*) Immunohistochemical analysis of AR in the hearts from a control subject, a DCM patient without *LMNA* mutation, and a DCM patient with p.R225X mutation. Immunostaining with anti-AR and -desmin antibodies shows localization of AR in the desmin-positive cardiomyocytes. Arrows indicate the representative nuclear accumulation of AR; scale bars=40 μm. Similar nuclear accumulation was found in two other DCM patients with the p.R225X. (*C*) Immunohistochemical analysis of AR in the hearts from $Lmna^{+/+}$ and $Lmna^{H222P/H222P}$ male mice at 6 months of age. Representative nuclear accumulation of AR was indicated as a high-magnification image. Nuclei in each tissue section were stained with DAPI; scale bars=40 μm. (*D* and *E*) Untransfected NRCs or NRCs transfected with GFP-tagged AR construct were treated with vehicle (0.01% ethanol), testosterone (1 μM), or testosterone (1 μM) plus flutamide (10 μM) 48 h after the transfection, fixed, and stained with DAPI and anti-SRF (*D*) or anti-FHL2 (*E*) antibody. Merged images are also shown. Arrows and arrowheads indicate the absence and presence, respectively, of GFP-AR in nuclei; scale bars=10 μm. Test +Flut; testosterone plus flutamide treated.

whereas the nuclear localization of AR was obviously increased in the heart samples from patients with p.R225X mutation (*Figure 3B*) and *Lmna*$^{H222P/H222P}$ mice (*Figure 3C* and see Supplementary material online, *Figure S3a*). We also investigated whether or not the nuclear accumulation of AR was observed in the hearts from GC-A KO mice[12] and TAC-operated mice,[13] because they were mouse models for cardiac hypertrophy, of which male mice showed more prominent cardiac phenotypes. However, no apparent change in the localization of AR was observed in both mouse models (see Supplementary material online, *Figure S4*), indicating that the nuclear AR accumulation in the cardiomyocytes was associated with specific *LMNA* mutations. In addition, accumulation of AR co-factors, SRF and FHL2, which are known to be involved in the cardiac remodelling,[20,21] was observed in the nuclei of hearts from the male patients with p.R225X (see Supplementary material online, *Figure S5*). Furthermore, the nuclear accumulation of SRF and FHL2 was observed in the hearts from male *Lmna*$^{H222P/H222P}$, but not from female mice (see Supplementary material online, *Figures S3* and *S6*). It was therefore confirmed *in vivo* that the nuclear accumulation of AR was accompanied by the nuclear translocation of SRF and FHL2 in male hearts with specific *LMNA* mutations.

3.4 Nuclear translocation of FHL2 and SRF in NRCs

The role of AR in nuclear accumulation of FHL2 and SRF was investigated in NRCs transfected with GFP-tagged AR in the presence or absence of testosterone or an AR antagonist, flutamide. GFP-AR and SRF were observed in both cytoplasm and nucleus (*Figure 2D*), while FHL2 was found specifically in the cytoplasm in the most (~90%) of transfected NRCs (*Figure 2E*). Upon treatment with testosterone, both GFP-AR and SRF translocated to nuclei, whereas FHL2 displayed partial nuclear localization in ~80% of the transfected NRCs. On the other hand, the testosterone-induced nuclear accumulation of AR, SRF, and FHL2 was suppressed by flutamide. In addition, silencing of *FHL2* by siRNA in NRCs expressing GFP-AR revealed that the preferential nuclear localization of SRF in testosterone-treated cells was mediated by FHL2 (*Figure 3*).

3.5 Survival prognosis of Lmna$^{H222P/H222P}$ mice with removal of gonadal organs

The role of sex hormones in the mortality and severity of *LMNA*-linked DCM was investigated *in vivo*, where male and female WT (*Lmna*$^{+/+}$) and *Lmna*$^{H222P/H222P}$ mice were castrated and ovariectomized, respectively (see Supplementary material online, *Figure S7*). We found that the castration significantly improved survival prognosis of male *Lmna*$^{H222P/H222P}$ mice, as evidenced by the prolonged 50% survival time (8.09 $\pm$ 0.27 vs. 10.25 $\pm$ 0.38 months, $P < 0.001$) and reduced overall mortality ($P < 0.001$, log-rank test) (*Figure 4A*). Improvement in mortality observed with ovariectomized *Lmna*$^{H222P/H222P}$ female mice was not statistically significant ($P = 0.10$), but the 50% survival time was significantly prolonged by the ovariectomy (10.10 $\pm$ 0.28 vs. 11.07 $\pm$ 0.32 months, $P < 0.05$) (*Figure 4A*). These data demonstrated the beneficial effect of removing gonadal organs on the survival prognosis of *Lmna*$^{H222P/H222P}$ mice especially in male mice and to only a little extent in female mice.

3.6 Evaluation of cardiac function in Lmna$^{H222P/H222P}$ mice with removal of gonadal organs

Cardiac function was evaluated by using transthoracic echocardiography for sham-operated and operated mice at 3–4, 6–7, and 9–10 months of age (see Supplementary material online, *Figure S7*). The sham-operated *Lmna*$^{H222P/H222P}$ mice, in both male and female, showed progressive LV dilation and contractile dysfunction, as indicated by the decreased LV fractional shortening (LVFS) and LV ejection fraction (LVEF). The castration preserved LVFS and LVEF in males, whereas the ovariectomy showed no significant impact in females (*Table 1*, see Supplementary material online, *Figure S8*). When we measured blood pressure of sham-operated and castrated *Lmna*$^{H222P/H222P}$ male mice at 4 months of age by the indirect tail-cuff method, the systolic blood pressure was not significantly changed by the castration; sham-operated 121.0 $\pm$ 3.7 vs. castrated 126.2 $\pm$ 4.0 mmHg ($n = 6$ in each group). These data demonstrated that the castration improved LV contractile dysfunction without affecting systolic blood pressure in the *Lmna*$^{H222P/H222P}$ mice. As for data of ECG, QRS complex duration and PR interval were prolonged, albeit not significant, in the *Lmna*$^{H222P/H222P}$ mice, in both male and female, as reported previously,[10] but there were no changes by the castration or ovariectomy (see Supplementary material online, *Table S3*).

To directly demonstrate the role of androgen in disease progression, we treated mice with testosterone or flutamide. By the testosterone treatment, cardiac dysfunction was accelerated in the castrated male *Lmna*$^{H222P/H222P}$ mice. In contrast, progression of cardiac dysfunction was slowed in the flutamide-treated male *Lmna*$^{H222P/H222P}$ mice (*Table 2*).

3.7 Histopathological study of hearts from Lmna$^{H222P/H222P}$ mice

Histopathological analyses of the hearts demonstrated the ventricular dilation with enlarged atrial cavity often accompanied by atrial thrombus in the sham-*Lmna*$^{H222P/H222P}$ mice. These abnormalities were also observed in the testosterone-treated female *Lmna*$^{H222P/H222P}$ mice as well as in the castrated and testosterone-treated male *Lmna*$^{H222P/H222P}$ mice (*Figure 4B*). Either castration or flutamide treatment prevented the development of CHF with congestive lung in the male *Lmna*$^{H222P/H222P}$ mice. Prominent interstitial fibrosis, degeneration, and necrosis of single and/or a small cluster of cardiomyocytes were found in the ventricles of sham-operated male *Lmna*$^{H222P/H222P}$, testosterone-treated castrated male *Lmna*$^{H222P/H222P}$, and testosterone-treated female *Lmna*$^{H222P/H222P}$ mice, but these abnormalities were suppressed in the castrated or flutamide-treated mice (*Figure 4B*). In addition, quantitative analyses of myocardial interstitial fibrosis demonstrated that the collagen deposits were significantly increased in the hearts from sham-operated male *Lmna*$^{H222P/H222P}$ mice, which was significantly suppressed by the castration or flutamide treatment (*Figure 4C* and *D*). These observations indicated that deprivation or blockage of testosterone-related signals inhibited the interstitial fibrosis in the *Lmna*$^{H222P/H222P}$ hearts.

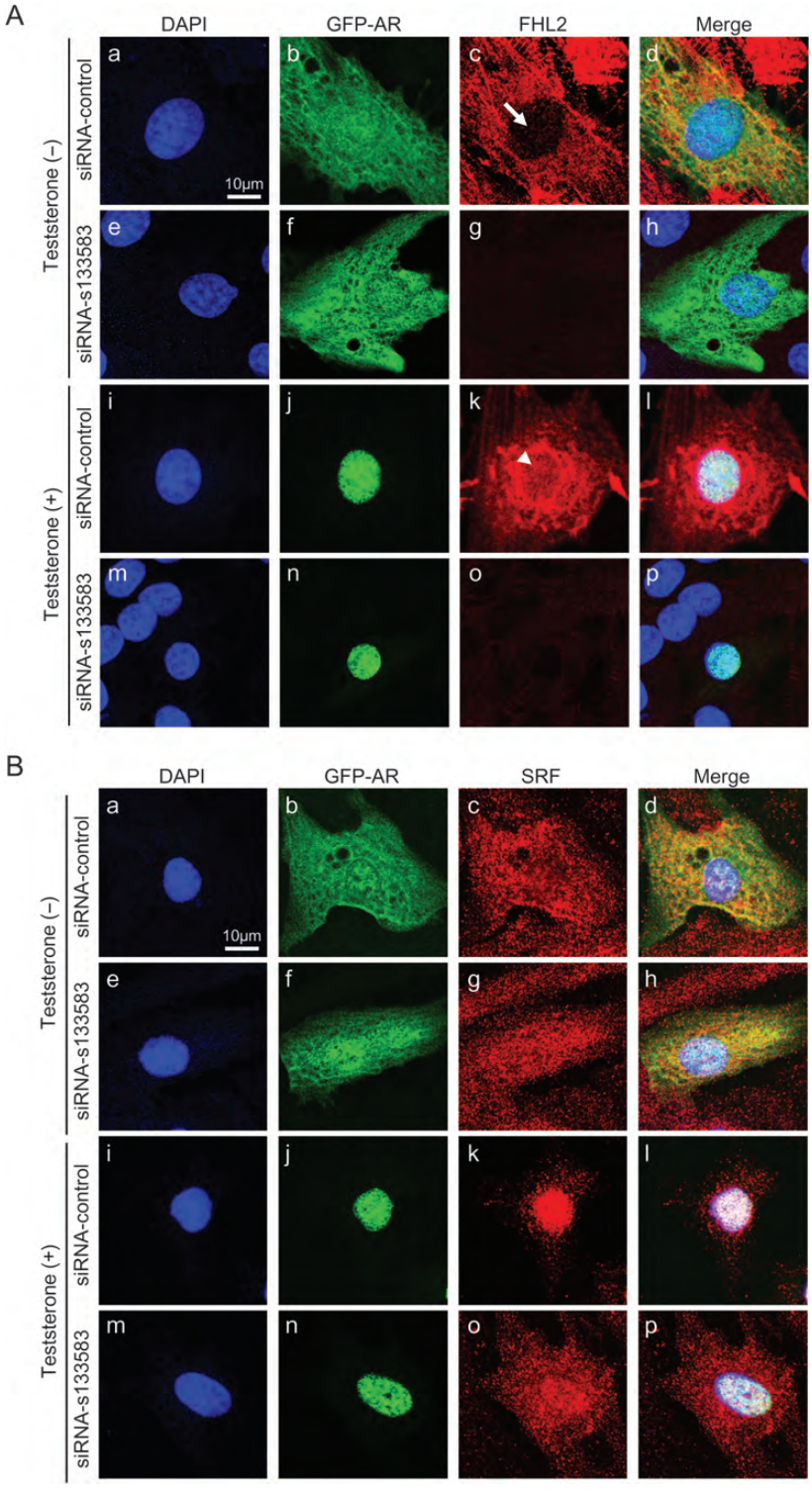

Figure 3 Effect of FHL2 silencing on localization of SRF in NRCs transiently expressed GFP-tagged AR and treated with testosterone. NRCs co-transfected with GFP-tagged AR construct and non-silencing (*a–d and i–l*), or pre-designed (e–*h* and *m–p*) siRNA were treated without (*a–d* and e–*h*) or with (*i–l* and *m–p*) testosterone (1 μM) 48 h after the transfection. The cells were fixed and stained with DAPI (*a*, e, *i*, and *m*) and anti-FHL2 (*c*, *g*, *k*, and *o* in *A*) or anti-SRF (*c*, *g*, *k*, and *o* in *B*) antibody. Merged images are shown in *d, h, l*, and *p*. Arrow and arrowhead indicate the absence and presence, respectively, of FHL2 in nuclei; scale bars=10 μm.

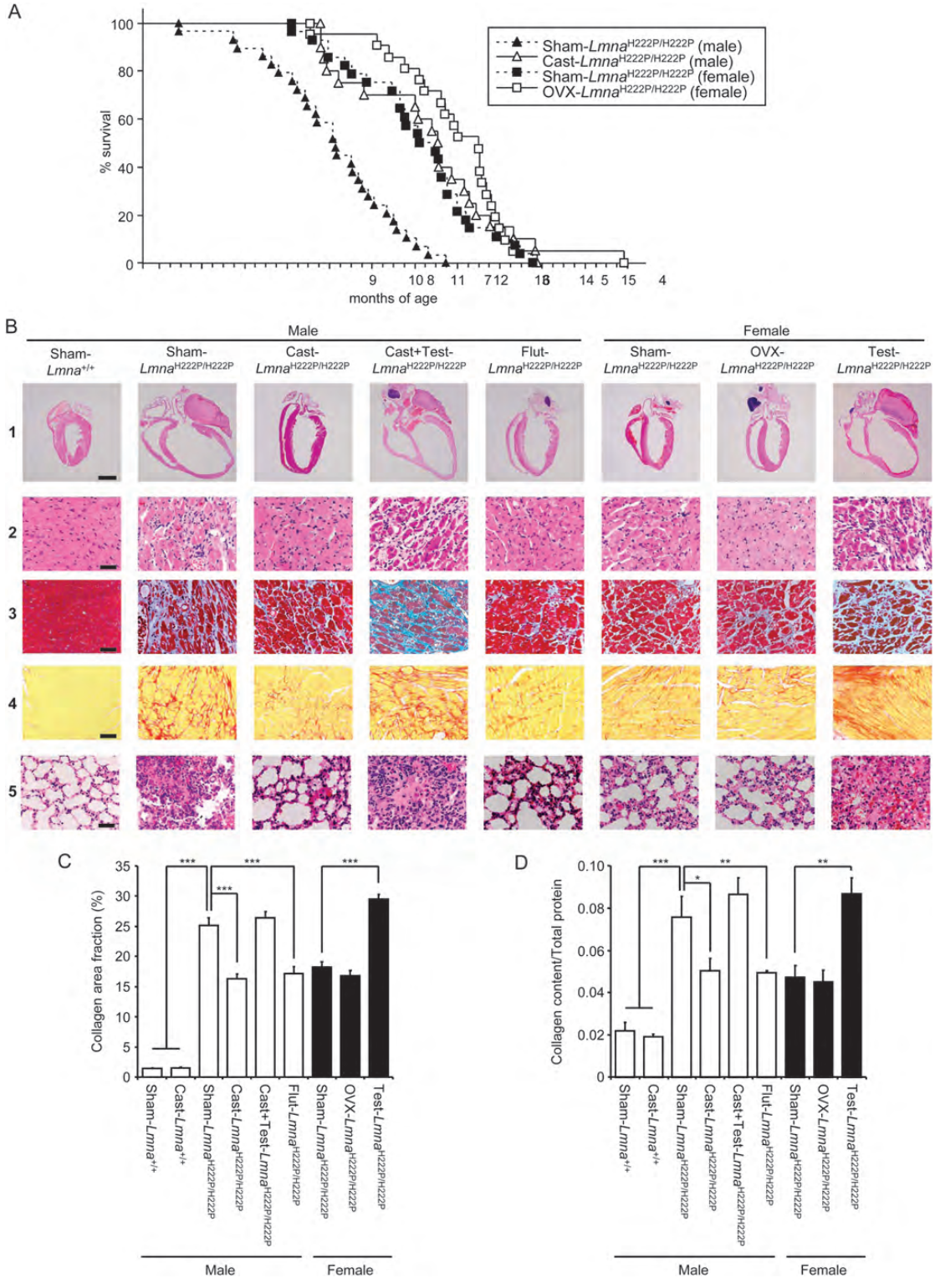

Figure 4 Disease expression of sham-operated and operated *Lmna*$^{H222P/H222P}$ mice. (*A*) Cumulative survival curves are indicated for sham-operated (Sham) male (closed triangles, $n = 29$) and female (closed squares, $n = 28$) mice, and castrated (Cast) male (open triangles, $n = 20$) and ovariectomized (OVX) female (open squares, $n = 21$) mice. (*B*) Pathological analyses of heart and lung; (1) longitudinal sections through the atria and ventricles of male and female mice at 6 months of age; scale bar=2 mm. Histopathological analysis of the LV with H&E staining (2), Masson's trichrome staining (3), or picrosirius red staining (4) and the lung with H&E staining (5); scale bars=50 μm except that in (4) =100 μm. (*C*) Quantitative measurement of myocardial collagen area fraction from five pictures per cross-section expressed as percentage of collagen staining to total area. Data are represented as means ± SEM for $n = 4$ to 6 per group. (*D*) Quantitative analysis of collagen content in the ventricles. Data are represented as means ± SEM for $n = 4$ to 6 per group. $^{*}P < 0.05$, $^{**}P < 0.01$, and $^{***}P < 0.001$. Sham: sham-operated, Cast: castrated, Cast+Test: castrated and testosterone-treated, Flut: flutamide-treated.

Table 1 Echocardiographic data for sham-operated and operated Lmna$^{+/+}$ and Lmna$^{H222P/H222P}$ mice

	IVSd (mm)	PWd (mm)	LVM (mg)	LVEDD (mm)	LVESD (mm)	LVFS (%)	LVEF (%)	Heart rate (beats/min)
Data for male mice aged 3–4, 6–7, and 9–10 months								
3–4 months of age								
Sham-*Lmna*$^{+/+}$ ($n = 12$)	0.47 ± 0.01	0.52 ± 0.02	38.3 ± 2.40	2.99 ± 0.07	1.74 ± 0.04	41.7 ± 0.70	79.4 ± 0.66	481 ± 18
Cast-*Lmna*$^{+/+}$ ($n = 13$)	0.48 ± 0.01	0.50 ± 0.02	31.4 ± 2.05	2.68 ± 0.09	1.60 ± 0.05	40.4 ± 0.51	78.3 ± 0.60	471 ± 12
Sham-*Lmna*$^{H222P/H222P}$ ($n = 15$)	0.50 ± 0.01	0.49 ± 0.02	44.7 ± 2.08	3.27 ± 0.09*	2.33 ± 0.10***	28.9 ± 1.32***	62.6 ± 1.85***	471 ± 12
Cast-*Lmna*$^{H222P/H222P}$ ($n = 15$)	0.48 ± 0.01	0.47 ± 0.02	39.3 ± 3.22	3.13 ± 0.11††	2.09 ± 0.09†††	33.2 ± 1.35†††,#	69.4 ± 1.73†††,#	511 ± 15
6–7 months of age								
Sham-*Lmna*$^{+/+}$ ($n = 12$)	0.48 ± 0.01	0.54 ± 0.03	46.4 ± 2.14	3.27 ± 0.06	1.80 ± 0.06	45.2 ± 1.28	82.1 ± 1.12	488 ± 11
Cast-*Lmna*$^{+/+}$ ($n = 13$)	0.48 ± 0.01	0.51 ± 0.02	39.2 ± 1.84	3.03 ± 0.09	1.76 ± 0.07	42.1 ± 1.04	80.0 ± 1.04	480 ± 11
Sham-*Lmna*$^{H222P/H222P}$ ($n = 15$)	0.48 ± 0.02	0.45 ± 0.02	58.4 ± 3.10	3.98 ± 0.11***	3.28 ± 0.13***	18.0 ± 1.18***	45.0 ± 2.46***	517 ± 17
Cast-*Lmna*$^{H222P/H222P}$ ($n = 14$)	0.47 ± 0.03	0.46 ± 0.02	41.9 ± 2.93##	3.30 ± 0.06†,###	2.34 ± 0.07†††,##	29.2 ± 1.23†††,###	63.5 ± 1.71†††,###	518 ± 14
9–10 months of age								
Sham-*Lmna*$^{+/+}$ ($n = 12$)	0.54 ± 0.02	0.54 ± 0.03	52.9 ± 3.26	3.38 ± 0.05	1.91 ± 0.03	43.5 ± 0.91	81.0 ± 0.85	494 ± 10
Cast-*Lmna*$^{+/+}$ ($n = 13$)	0.48 ± 0.02	0.53 ± 0.02	41.4 ± 2.04	3.08 ± 0.08	1.78 ± 0.06	43.9 ± 1.05	81.5 ± 1.11	506 ± 12
Sham-*Lmna*$^{H222P/H222P}$ ($n = 5$)	0.39 ± 0.02**	0.33 ± 0.03**	54.1 ± 4.98	4.51 ± 0.22***	3.93 ± 0.23***	12.9 ± 1.79***	33.9 ± 4.41***	484 ± 21
Cast-*Lmna*$^{H222P/H222P}$ ($n = 12$)	0.47 ± 0.01##	0.47 ± 0.03†††,##	52.4 ± 1.46†	3.72 ± 0.14†††,##	2.97 ± 0.17†††,##	20.9 ± 1.86†††,#	50.2 ± 3.59†††,#	533 ± 14
Data for female mice aged 3–4, 6–7, and 9–10 months								
3–4 months of age								
Sham-*Lmna*$^{+/+}$ ($n = 10$)	0.44 ± 0.01	0.48 ± 0.03	31.7 ± 1.43	2.83 ± 0.08	1.61 ± 0.07	43.3 ± 1.98	80.5 ± 1.72	531 ± 16
OVX-*Lmna*$^{+/+}$ ($n = 11$)	0.48 ± 0.01	0.49 ± 0.03	32.4 ± 2.63	2.75 ± 0.07	1.58 ± 0.05	42.8 ± 1.03	80.6 ± 1.01	514 ± 18
Sham-*Lmna*$^{H222P/H222P}$ ($n = 13$)	0.46 ± 0.02	0.46 ± 0.02	38.6 ± 2.74	3.17 ± 0.12*	2.15 ± 0.12**	32.7 ± 1.51***	68.4 ± 2.12***	508 ± 13
OVX-*Lmna*$^{H222P/H222P}$ ($n = 15$)	0.50 ± 0.02	0.49 ± 0.02	34.5 ± 2.03	2.81 ± 0.08#	1.87 ± 0.07††	32.9 ± 1.53†††	68.9 ± 2.30†††	473 ± 9
6–7 months of age								
Sham-*Lmna*$^{+/+}$ ($n = 9$)	0.44 ± 0.01	0.49 ± 0.04	38.9 ± 1.71	3.16 ± 0.07	1.86 ± 0.04	41.3 ± 0.35	78.8 ± 0.44	483 ± 13
OVX-*Lmna*$^{+/+}$ ($n = 11$)	0.50 ± 0.01	0.51 ± 0.02	43.9 ± 1.98	3.19 ± 0.06	1.83 ± 0.05	42.7 ± 0.84	80.4 ± 0.74	487 ± 18
Sham-*Lmna*$^{H222P/H222P}$ ($n = 13$)	0.45 ± 0.01	0.51 ± 0.02	42.3 ± 1.67	3.24 ± 0.08	2.33 ± 0.10***	28.3 ± 1.70***	61.8 ± 2.45***	515 ± 10
OVX-*Lmna*$^{H222P/H222P}$ ($n = 15$)	0.47 ± 0.01	0.47 ± 0.02	40.7 ± 1.83	3.22 ± 0.05	2.35 ± 0.05†††	27.3 ± 0.84†††	60.5 ± 1.32†††	488 ± 11
9–10 months of age								
Sham-*Lmna*$^{+/+}$ ($n = 9$)	0.52 ± 0.02	0.58 ± 0.04	50.1 ± 2.90	3.23 ± 0.09	1.86 ± 0.06	44.9 ± 1.75	82.2 ± 1.45	486 ± 12
OVX-*Lmna*$^{+/+}$ ($n = 10$)	0.52 ± 0.01	0.55 ± 0.04	48.3 ± 4.66	3.23 ± 0.12	1.84 ± 0.07	43.2 ± 0.97	80.8 ± 1.00	527 ± 11
Sham-*Lmna*$^{H222P/H222P}$ ($n = 9$)	0.46 ± 0.03	0.47 ± 0.03**	56.0 ± 3.10	3.91 ± 0.18**	3.18 ± 0.21***	19.1 ± 2.11***	46.7 ± 3.86***	506 ± 14
OVX-*Lmna*$^{H222P/H222P}$ ($n = 13$)	0.47 ± 0.01	0.45 ± 0.03	46.6 ± 2.06	3.53 ± 0.09	2.76 ± 0.11†††	22.6 ± 1.63†††	52.2 ± 2.85†††	519 ± 13

Cardiac function was evaluated by transthoracic echocardiographic analyses of the left ventricle (LV): the left ventricular mass (LVM) and the percentage of left ventricular ejection fraction (LVEF) and fractional shortening (LVFS) were calculated as follows: [(IVSd+PWd+EDD)3−EDD3] × 1.055 and (LVEDD-LVESD)/LVEDD x 100, respectively.
IVSd, interventricular septal wall thickness in diastole; LVEDD, left ventricular end-diastolic diameter; LVEF, left ventricular ejection fraction; LVESD, left ventricular end-systolic diameter; PWd, posterior wall thickness in diastole.
*$P < 0.05$, **$P < 0.01$, and ***$P < 0.001$, vs. age- and sex-matched Sham-Lmna+/+ mice.
†$P < 0.05$, ††$P < 0.01$, and †††$P < 0.001$, vs. age- and sex-matched Cast- or OVX-Lmna+/+ mice.
#$P < 0.05$, ##$P < 0.01$, and ###$P < 0.001$, vs. age- and sex-matched Sham-LmnaH222P/H222P mice.

Table 2 Echocardiographic data from *Lmna*$^{+/+}$ and *Lmna*$^{H222P/H222P}$ mice treated with testosterone or flutamide

	IVSd (mm)	PWd (mm)	LVM (mg)	LVEDD (mm)	LVESD (mm)	LVFS (%)	LVEF (%)	Heart rate (bpm)
Data for mice aged 4 months								
Sham-*Lmna*$^{+/+}$ (male, $n = 5$)	0.55 ± 0.02	0.51 ± 0.02	45.0 ± 3.50	3.12 ± 0.09	1.71 ± 0.09	43.9 ± 0.57	81.4 ± 0.61	511 ± 26
Cast+Testosterone-*Lmna*$^{+/+}$ (male, $n = 5$)	0.53 ± 0.02	0.51 ± 0.02	42.5 ± 2.84	3.06 ± 0.13	1.64 ± 0.05	44.1 ± 0.97	82.2 ± 0.88	496 ± 5
Flutamide-*Lmna*$^{+/+}$ (male, $n = 5$)	0.51 ± 0.03	0.54 ± 0.03	45.7 ± 5.19	3.17 ± 0.09	1.71 ± 0.05	43.0 ± 0.25	80.5 ± 0.18	528 ± 3
Sham-*Lmna*$^{H222P/H222P}$ (male, $n = 19$)	0.52 ± 0.01	0.52 ± 0.02	51.1 ± 2.52	3.41 ± 0.08	2.45 ± 0.07	28.1 ± 0.78	62.2 ± 1.14	492 ± 13
Cast-*Lmna*$^{H222P/H222P}$ (male, $n = 14$)	0.48 ± 0.01	0.56 ± 0.02	48.6 ± 2.55	3.31 ± 0.07	2.27 ± 0.06	32.7 ± 0.76***	69.0 ± 0.92***	523 ± 15
Cast+Testosterone-*Lmna*$^{H222P/H222P}$ (male, $n = 14$)	0.52 ± 0.02	0.55 ± 0.04	50.7 ± 3.76	3.32 ± 0.05	2.21 ± 0.05*	33.4 ± 0.74***	69.0 ± 0.98***	521 ± 13
Flutamide-*Lmna*$^{H222P/H222P}$ (male, $n = 10$)	0.53 ± 0.01	0.55 ± 0.02	55.3 ± 2.79	3.47 ± 0.05	2.47 ± 0.04	28.8 ± 0.39	63.5 ± 0.46	547 ± 11
Sham-*Lmna*$^{+/+}$ (female, $n = 5$)	0.43 ± 0.02	0.54 ± 0.03	37.7 ± 4.08	3.01 ± 0.08	1.67 ± 0.05	43.1 ± 0.63	80.8 ± 0.67	544 ± 8
Testosterone-*Lmna*$^{+/+}$ (female, $n = 5$)	0.46 ± 0.02	0.55 ± 0.02	41.4 ± 2.86	3.08 ± 0.04	1.68 ± 0.02	42.7 ± 0.52	80.9 ± 0.60	564 ± 7
Sham-*Lmna*$^{H222P/H222P}$ (female, $n = 17$)	0.48 ± 0.02	0.56 ± 0.02	45.9 ± 2.11	3.20 ± 0.09	2.22 ± 0.09	32.9 ± 0.74	68.5 ± 1.61	516 ± 11
Testosterone-*Lmna*$^{H222P/H222P}$ (female, $n = 10$)	0.51 ± 0.02	0.56 ± 0.03	47.6 ± 3.43	3.20 ± 0.03	2.24 ± 0.02	32.0 ± 0.66	67.7 ± 0.75	537 ± 12
Data for mice aged 6 months								
Sham-*Lmna*$^{+/+}$ (male, $n = 5$)	0.52 ± 0.04	0.57 ± 0.06	49.5 ± 7.45	3.23 ± 0.06	1.82 ± 0.04	43.7 ± 0.44	81.4 ± 0.41	551 ± 16
Cast+Testosterone-*Lmna*$^{+/+}$ (male, $n = 5$)	0.52 ± 0.02	0.59 ± 0.05	48.3 ± 3.95	3.14 ± 0.06	1.76 ± 0.05	42.2 ± 0.45	80.2 ± 0.48	511 ± 3
Flutamide-*Lmna*$^{+/+}$ (male, $n = 5$)	0.51 ± 0.02	0.60 ± 0.03	50.2 ± 5.28	3.21 ± 0.09	1.82 ± 0.05	43.5 ± 0.32	81.4 ± 0.28	526 ± 8
Sham-*Lmna*$^{H222P/H222P}$ (male, $n = 15$)	0.44 ± 0.02	0.45 ± 0.02	53.4 ± 2.77	3.90 ± 0.11	3.19 ± 0.14	18.7 ± 1.40	46.3 ± 2.63	540 ± 15
Cast-*Lmna*$^{H222P/H222P}$ (male, $n = 13$)	0.44 ± 0.01	0.50 ± 0.02	48.1 ± 2.72	3.54 ± 0.08*	2.53 ± 0.08***	28.5 ± 0.91***	62.7 ± 1.21***	505 ± 14
Cast+Testosterone-*Lmna*$^{H222P/H222P}$ (male, $n = 10$)	0.42 ± 0.03	0.42 ± 0.03	56.7 ± 2.80	4.19 ± 0.12	3.46 ± 0.13	17.5 ± 1.36	44.0 ± 2.89	504 ± 9
Flutamide-*Lmna*$^{H222P/H222P}$ (male, $n = 8$)	0.47 ± 0.02	0.48 ± 0.03	49.9 ± 2.98	3.59 ± 0.05	2.62 ± 0.05**	26.9 ± 0.57***	61.6 ± 0.93***	553 ± 14
Sham-*Lmna*$^{+/+}$ (female, $n = 5$)	0.48 ± 0.01	0.57 ± 0.02	45.9 ± 2.63	3.18 ± 0.06	1.85 ± 0.03	42.0 ± 0.20	80.1 ± 0.18	547 ± 7
Testosterone-*Lmna*$^{+/+}$ (female, $n = 5$)	0.47 ± 0.01	0.61 ± 0.04	46.9 ± 3.55	3.15 ± 0.05	1.79 ± 0.02	43.1 ± 0.36	80.8 ± 0.37	576 ± 17
Sham-*Lmna*$^{H222P/H222P}$ (female, $n = 17$)	0.48 ± 0.01	0.50 ± 0.02	44.6 ± 1.67	3.29 ± 0.06	2.37 ± 0.07	28.3 ± 1.28	62.0 ± 1.86	529 ± 11
Testosterone-*Lmna*$^{H222P/H222P}$ (female, $n = 9$)	0.39 ± 0.03	0.39 ± 0.03	47.3 ± 4.87	3.98 ± 0.13***	3.21 ± 0.14***	19.5 ± 1.23***	48.4 ± 2.33***	528 ± 18

Cardiac function was evaluated by transthoracic echocardiographic analyses of the left ventricle (LV): the left ventricular mass (LVM) and the percentage of left ventricular ejection fraction (LVEF) and fractional shortening (LVFS) were calculated as follows: [(IVSd+PWd+EDD)3−EDD3] × 1.055 and (LVEDD-LVESD)/LVEDD × 100, respectively.
IVSd, interventricular septal wall thickness in diastole; LVEDD, left ventricular end-diastolic diameter; LVEF, left ventricular ejection fraction; LVESD, left ventricular end-systolic diameter; PWd, posterior wall thickness in diastole.
*$P < 0.05$, **$P < 0.01$, and ***$P < 0.001$, vs. age-, sex-, and genotype-matched Sham-operated mice.

3.8 Altered expression of genes and proteins related with cardiac remodelling in hearts from Lmna$^{H222P/H222P}$ mice

Abnormal regulation of gene or protein expression involved in the sarcomere organization, cardiac hormones, proto-oncogene, and extracellular matrix remodelling is associated with DCM and CHF,[22] and SRF is required for the induction of cardiac remodelling-associated genes including *Nppa*, *Nppb*, *Myh7*, and *Fos*.[20] We investigated the gene expression profiles in the hearts from *Lmna*$^{H222P/H222P}$ mice. It was observed that the expression of *Nppa*, *Nppb*, and *Myh7* at the mRNA level was increased in the hearts from sham-operated male *Lmna*$^{H222P/H222P}$ mice, and that the up-regulation was suppressed in the hearts from castrated or flutamide-treated male *Lmna*$^{H222P/H222P}$ mice (*Figure 5*). In addition, significant increase in expression of proto-oncogene *Fos* and extracellular matrix remodelling-related genes, such as *Tgfb1*, *Tgfb2*, and *Col1a2*, was found in the hearts from the sham-operated male *Lmna*$^{H222P/H222P}$ mice, which were suppressed by the castration or flutamide treatment (*Figure 5*). Expression of *Nppa*, *Nppb*, *Myh7*, and *Col1a2* was significantly increased in the hearts from testosterone-treated female *Lmna*$^{H222P/H222P}$ mice (*Figure 5*). Moreover, altered expression of atrial natriuretic peptide and β-myosin heavy chain encoded by *Nppa* and *Myh7*, respectively, was confirmed at the protein levels (see Supplementary material online, *Figure S9*).

3.9 Accumulation of androgen-related proteins in nuclei of cardiomyocytes from Lmna$^{H222P/H222P}$ mice

Next, we investigated the expression of AR in the hearts from *Lmna*$^{+/+}$ and *Lmna*$^{H222P/H222P}$ mice (*Table 2*). Western blot analyses showed an increased expression of AR in both total protein and nuclear extracts from the *Lmna*$^{H222P/H222P}$ hearts, irrespective of gender (*Figure 6A* and *B*). The nuclear accumulation of AR was accompanied by the AR co-factors, SRF and FHL2, in the male *Lmna*$^{H222P/H222P}$ hearts, but not in the female *Lmna*$^{H222P/H222P}$ hearts (*Figure 6C* and *D*). The increased nuclear accumulation of SRF and FHL2 was suppressed in the castrated male *Lmna*$^{H222P/H222P}$ mice, whereas no difference was observed in the expression of AR between sham-operated and castrated male *Lmna*$^{H222P/H222P}$ mice (*Figure 6C*). On the other hand, no nuclear accumulation of AR, SRF, or FHL2 was observed in the soleus muscle from the *Lmna*$^{H222P/H222P}$ mice (see Supplementary material online, *Figure S10*). These observations suggested that the nuclear accumulation of androgen-related proteins was specific to the heart muscle, not the skeletal muscles, in *Lmna*$^{H222P/H222P}$ mice, which was consistent with the findings that the gender difference was observed only for cardiac function and not for skeletal muscle symptoms in the *Lmna*$^{H222P/H222P}$ mice.[10]

4. Discussion

Sex hormones mediate their function by activation of specific receptors. Upon activation, sex hormone receptors translocate into nuclei, where they bind hormone response elements in the regulatory region of target genes, and, together with co-activators and other transcription factors, initiate transcription. In this context, androgens including testosterone mediate their action via AR, and androgen-activated AR exerts its biological effect via complex formation with co-regulators.[23] In this study, we demonstrated the increased expression and nuclear accumulation of AR in the hearts from the DCM patients carrying the p.R225X mutation and the *Lmna*$^{H222P/H222P}$ mice. Quite interestingly, we found concomitantly nuclear accumulation of SRF and FHL2 in cardiomyocytes from the human DCM patients and mice. It was reported that SRF and FHL2 formed a complex with AR to act as co-activators of AR-dependent transcription.[24,25] SRF is required for the induction of cardiac remodelling-related genes including *Nppa*, *Nppb*, *Myh7*, and *Fos*,[20] of which expression was increased in the *Lmna*$^{H222P/H222P}$ hearts. In addition, FHL2 is preferentially expressed in the cardiac muscle and only a little in the skeletal muscles.[26] These observations suggested that the cardiomyocyte-specific nuclear accumulation of AR-FHL2-SRF complex induced by testosterone was involved in the disease progression of DCM caused by specific *LMNA* mutations. It is noteworthy that overexpression of AR accelerated nuclear accumulation of FHL2 and SRF in NRCs in the presence of testosterone, and silencing of FHL2 suppressed the translocation of SRF into the nuclei. It is therefore implied that a blockade of SRF–AR–FHL2 complex formation might be a therapeutic strategy for adverse effect of testosterone in DCM caused by *LMNA* mutation. It may be advocating that a high dose testosterone treatment might not be beneficial for CHF, especially for individuals whose AR expression would be increased in the heart, because nuclear accumulation of AR in the cardiac muscles is associated with higher mortality and severity of cardiac dysfunction.

Significant gender differences in morbidity and mortality of human CHF including DCM has been recognized.[6,27,28] Hormone-replacement therapy appeared to improve survival in post-menopausal women with systolic dysfunction.[29] In addition, it has been demonstrated that males displayed more prominent abnormalities in cardiac function than females, and female-related phenotypes could be mimicked by administration of estradiol in males and ovariectomized females in mice.[8] These observations suggested the role of oestrogen as a cardiac protector. On the other hand, potential influence of androgens on the cardiac hypertrophy and fibrosis in mice was described in some reports,[12,30] and a low dose testosterone supplementation improves cardiac functional capacity in CHF patients.[31] However, the adverse or beneficial role of androgens in cardiovascular risk is not fully understood. In this study, we revealed a deleterious role of testosterone in the progression of DCM in a mouse model caused by the *LMNA* mutations.

Castration significantly improved cardiac function and survival prognosis of the male *Lmna*$^{H222P/H222P}$ mice. Interestingly, ovariectomy also improved survival prognosis, albeit to less extent, of the female *Lmna*$^{H222P/H222P}$ mice. Because a small amount of testosterone is produced in the ovary, it was speculated that a slight improvement of survival prognosis in the ovariectomized female *Lmna*$^{H222P/H222P}$ mice was due to the elimination of ovarian testosterone. We also demonstrated that the testosterone significantly worsened the cardiac function in the castrated male *Lmna*$^{H222P/H222P}$ mice and female *Lmna*$^{H222P/H222P}$ mice, indicating the impact of testosterone on disease progression. Because the increased expression of AR was observed in the hearts from both male and female *Lmna*$^{H222P/H222P}$ mice, it was suggested that the presence of both testosterone and AR played pivotal roles in the cardiac phenotype of *Lmna*$^{H222P/H222P}$ mice.

The up-regulation of extracellular matrix remodelling-related genes in the male *Lmna*$^{H222P/H222P}$ mice was significantly suppressed by the castration or treatment with the AR antagonist. This finding was consistent with the significant inhibition of interstitial fibrosis in the hearts from castrated or flutamide-treated male *Lmna*$^{H222P/H222P}$ mice. On the other hand, a long-term treatment with testosterone increased the cardiac

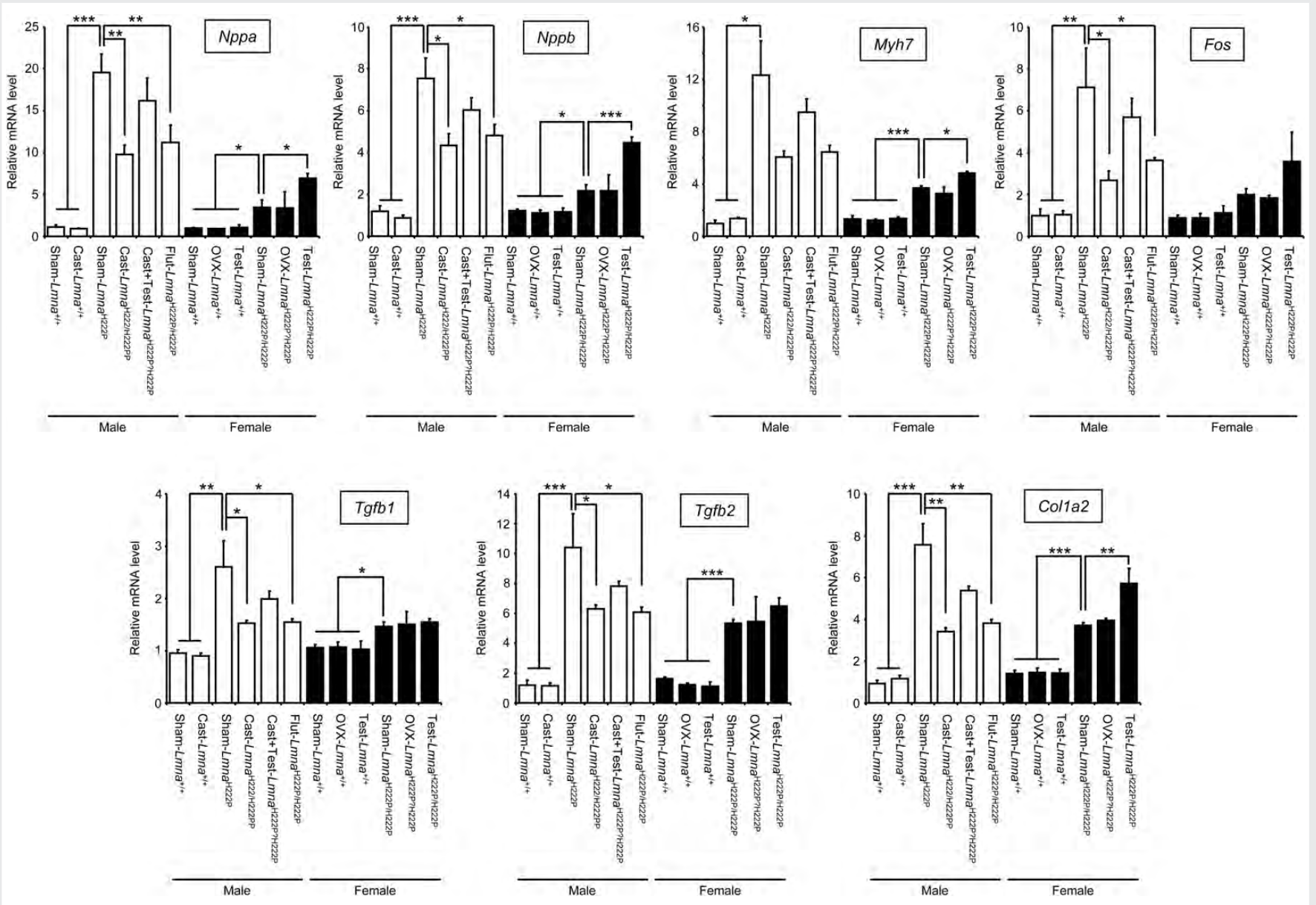

Figure 5 Expression of cardiac remodelling-related genes in LVs from $Lmna^{+/+}$ and $Lmna^{H222P/H222P}$ mice. Quantitative real-time RT–PCR data showing the steady-state mRNA levels of *Nppa*, *Nppb*, *Myh7*, *Fos*, *Tgfb1*, *Tgfb2*, and *Col1a2*, which encode for atrial natriuretic peptide precursor, brain natriuretic peptide precursor, β-myosin heavy chain, c-fos, TGF-β_1, TGF-β_2, and type I collagen α2 chain, respectively. Bars indicate the mRNA level in LVs normalized to *Gapdh* as calculated by the ΔδCT method. Data are arbitrarily shown as fold-induction and the expression of each gene in LV from a sham-operated $Lmna^{+/+}$ mouse was defined as 1.00 AU. Data are expressed as means ± SEM for $n = 6$ per group. Other marks and abbreviations are the same as in the legends to *Figure 4*.

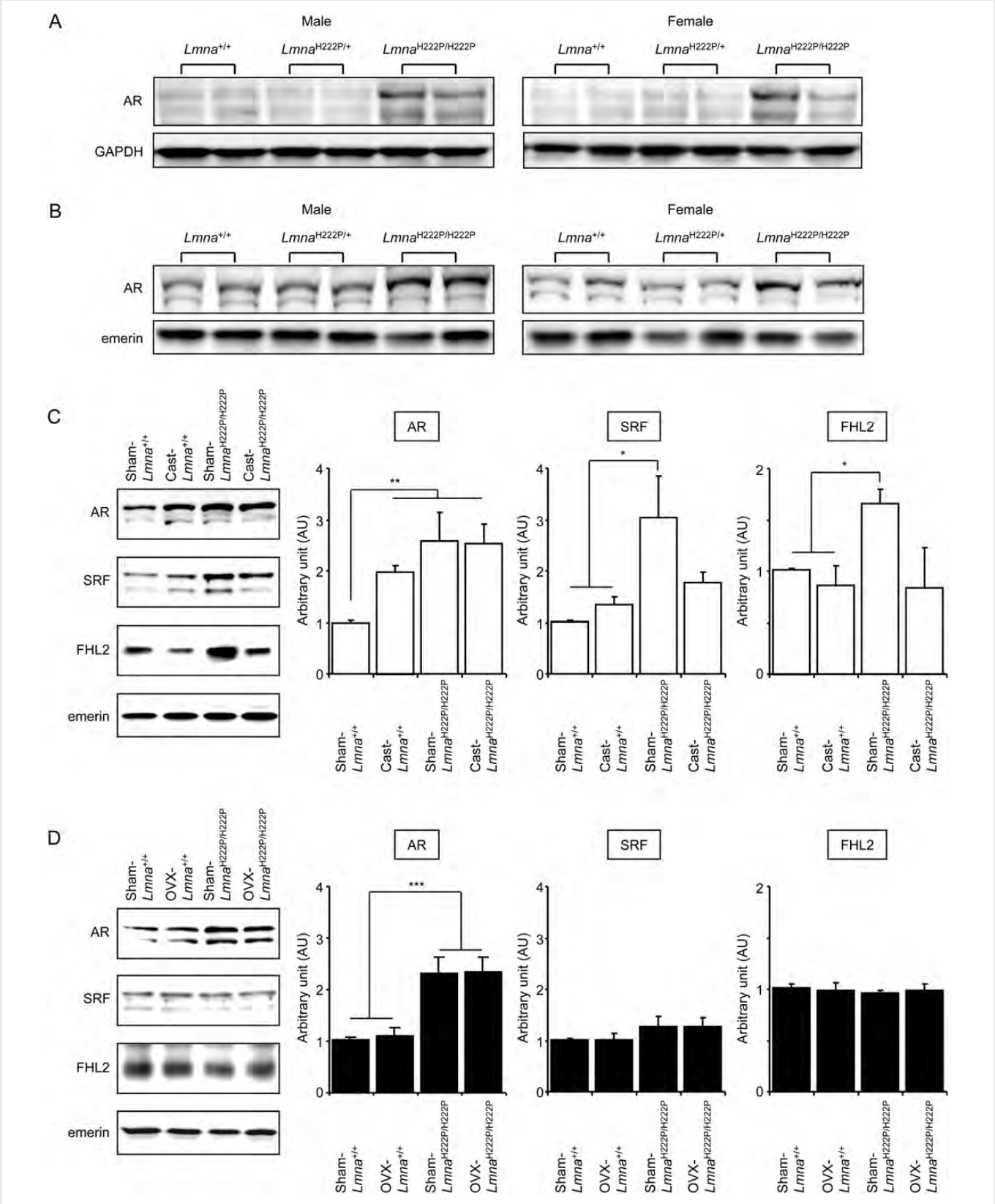

Figure 6 Expression of androgen-related proteins in LVs from mice at 6 months of age. (*A*) Representative immunoblots for AR in total protein extracts from LVs of male and female mice are shown. Labelling with antibody against GAPDH is shown as the loading control. (*B*) Representative immunoblots for AR in nuclear fraction from LV of male and female mice are shown. Labelling with antibody against a nuclear protein, emerin, is shown as the loading control. (*C* and *D*) Expression of AR, SRF, and FHL2 in the nuclear extracts from LVs of sham-operated and operated male (*C*) and female (*D*) mice. Labelling with antibody against emerin is shown as the loading control. Data are arbitrarily shown as fold-inductions and the expression of each protein in LV from a sham-operated $Lmna^{+/+}$ mouse was defined as 1.00 AU. Data are expressed as means ± SEM for $n = 4$ to 8 per group. Other marks and abbreviations are the same as in the legends to *Figure 4*.

fibrosis in the female *Lmna*$^{H222P/H222P}$ mice. It was previously reported that either castration or treatment with flutamide attenuated the cardiac fibrosis in GC-A KO mice.[12] However, nuclear accumulation of AR was not observed in the hearts from the GC-A KO mice in this study. These observations suggested that testosterone played a role in the cardiac remodelling including interstitial fibrosis, but molecular mechanisms underlying the gender difference in the cardiac dysfunction due to the *LMNA* mutations would be different from that caused by the knock-out of the GC-A gene.

There are some limitations in this study. First, it is not resolved how the specific *LMNA* mutations lead to the cardiomyocyte-specific nuclear accumulation of AR. Second, we have not evaluated the angiogenesis in the hearts, which is a hallmark of cardiac remodelling. These issues should be further investigated to elucidate the molecular mechanisms for the gender difference.

In conclusion, we revealed that the nuclear accumulation of AR–FHL2–SRF complex was associated with specific *LMNA* mutations showing the gender difference in disease progression of DCM. We also demonstrated a deleterious effect of testosterone on the DCM phenotypes and survival prognosis in the *Lmna*$^{H222P/H222P}$ mice. Our findings implicated that a blockade of AR signalling might be beneficial for preserving cardiac function in the DCM patients, when nuclear accumulation of AR could be found in their hearts. Nuclear AR accumulation could be a biomarker for prediction of harmful side effects in testosterone supplement therapy for CHF.[31]

Supplementary material

Supplementary material is available at *Cardiovascular Research* online.

Acknowledgements

We are grateful to Prof. K. Taya for helpful discussion about the use of silascon tubes in infusion of testosterone and flutamide. We also thank SRL, Inc. for measuring serum testosterone levels in mice.

Conflict of interest: none declared.

Funding

This work was supported in part by Grant-in-Aids from the Ministry of Education, Culture, Sports, Science and Technology, Japan (grant numbers 22390157, 23132507); grants for Japan–France collaboration research from the Japan Society for the Promotion of Science (JSPS) and the '*Institut National de la Santé et de la Recherche Médicale*' (Inserm); a research grant for Intractable Disease from the Ministry of Health, Labour and Welfare, Japan (grant number 2010-119); a research grant from the 'Association Française contre les Myopathies' (AFM) (grant number 15261); a Grant-in-Aid for SENTAN from the Japan Science and Technology Agency; and the Follow-up grants from the Tokyo Medical and Dental University. This work was also supported by Joint Usage/Research Program of Medical Research Institute, Tokyo Medical and Dental University.

References

1. Richardson P, McKenna W, Bristow M, Maisch B, Mautner B, O'Connell J *et al*. Report of the 1995 World Health Organization/International Society and Federation of Cardiology Task Force on the Definition and Classification of cardiomyopathies. *Circulation* 1996;**93**:841–842.
2. Maron BJ, Towbin JA, Thiene G, Antzelevitch C, Corrado D, Arnett D *et al*. Contemporary definitions and classification of the cardiomyopathies: an American Heart Association Scientific Statement from the Council on Clinical Cardiology, Heart Failure and Transplantation Committee; Quality of Care and Outcomes Research and Functional Genomics and Translational Biology Interdisciplinary Working Groups; and Council on Epidemiology and Prevention. *Circulation* 2006;**113**:1807–1816.
3. Towbin JA, Lowe AM, Colan SD, Sleeper LA, Orav EJ, Clunie S *et al*. Incidence, causes, and outcomes of dilated cardiomyopathy in children. *JAMA* 2006;**296**:1867–1876.
4. Kimura A. Contribution of genetic factors to the pathogenesis of dilated cardiomyopathy: the cause of dilated cardiomyopathy: genetic or acquired? (genetic-side). *Circ J* 2011;**75**:1756–1765.
5. Taylor MR, Fain PR, Sinagra G, Robinson ML, Robertson AD, Carniel E *et al*. Natural history of dilated cardiomyopathy due to lamin A/C gene mutations. *J Am Coll Cardiol* 2003;**41**:771–780.
6. Towbin JA, Bowles NE. The failing heart. *Nature* 2002;**415**:227–233.
7. van Rijsingen IA, Nannenberg EA, Arbustini E, Elliott PM, Mogensen J, Ast JF *et al*. Gender-specific differences in major cardiac events and mortality in lamin A/C mutation carriers. *Eur J Heart Fail* 2013;**15**:376–384.
8. Du XJ. Gender modulates cardiac phenotype development in genetically modified mice. *Cardiovasc Res* 2004;**63**:510–519.
9. Babiker FA, De Windt LJ, van Eickels M, Grohe C, Meyer R, Doevendans PA. Estrogenic hormone action in the heart: regulatory network and function. *Cardiovasc Res* 2002;**53**:709–719.
10. Arimura T, Helbling-Leclerc A, Massart C, Varnous S, Niel F, Lacene E *et al*. Mouse model carrying H222P-Lmna mutation develops muscular dystrophy and dilated cardiomyopathy similar to human striated muscle laminopathies. *Hum Mol Genet* 2005;**14**:155–169.
11. Bertrand AT, Renou L, Papadopoulos A, Beuvin M, Lacene E, Massart C *et al*. DelK32-lamin A/C has abnormal location and induces incomplete tissue maturation and severe metabolic defects leading to premature death. *Hum Mol Genet* 2012;**21**:1037–1048.
12. Li Y, Kishimoto I, Saito Y, Harada M, Kuwahara K, Izumi T *et al*. Androgen contributes to gender-related cardiac hypertrophy and fibrosis in mice lacking the gene encoding guanylyl cyclase-A. *Endocrinology* 2004;**145**:951–958.
13. Montalvo C, Villar AV, Merino D, Garcia R, Ares M, Llano M *et al*. Androgens contribute to sex differences in myocardial remodeling under pressure overload by a mechanism involving TGF-beta. *PLoS ONE* **7**:e35635.
14. Arimura T, Bos JM, Sato A, Kubo T, Okamoto H, Nishi H *et al*. Cardiac ankyrin repeat protein gene (ANKRD1) mutations in hypertrophic cardiomyopathy. *J Am Coll Cardiol* 2009;**54**:334–342.
15. Purevjav E, Arimura T, Augustin S, Huby AC, Takagi K, Nunoda S *et al*. Molecular basis for clinical heterogeneity in inherited cardiomyopathies due to myopalladin mutations. *Hum Mol Genet* 2012;**21**:2039–2053.
16. Li C, Taneda S, Suzuki AK, Furuta C, Watanabe G, Taya K. Anti-androgenic activity of 3-methyl-4-nitrophenol in diesel exhaust particles. *Eur J Pharmacol* 2006;**543**:194–199.
17. Kuwahara M, Chiku K, Shiono T, Tsubone H, Sugano S. ECG changes under hyperkalemia with nephrectomy in the rat. *J Electrocardiol* 1992;**25**:215–219.
18. Arimura T, Sato R, Machida N, Bando H, Zhan DY, Morimoto S *et al*. Improvement of left ventricular dysfunction and of survival prognosis of dilated cardiomyopathy by administration of calcium sensitizer SCH00013 in a mouse model. *J Am Coll Cardiol* 2010;**55**:1503–1505.
19. Muchir A, Pavlidis P, Decostre V, Herron AJ, Arimura T, Bonne G *et al*. Activation of MAPK pathways links LMNA mutations to cardiomyopathy in Emery-Dreifuss muscular dystrophy. *J Clin Invest* 2007;**117**:1282–1293.
20. Nelson TJ, Balza R Jr, Xiao Q, Misra RP. SRF-dependent gene expression in isolated cardiomyocytes: regulation of genes involved in cardiac hypertrophy. *J Mol Cell Cardiol* 2005;**39**:479–489.
21. Niu Z, Li A, Zhang SX, Schwartz RJ. Serum response factor micromanaging cardiogenesis. *Curr Opin Cell Biol* 2007;**19**:618–627.
22. Margulies KB, Bednarik DP, Dries DL. Genomics, transcriptional profiling, and heart failure. *J Am Coll Cardiol* 2009;**53**:1752–1759.
23. Walters KA, Allan CM, Handelsman DJ. Androgen actions and the ovary. *Biol Reprod* 2008;**78**:380–389.
24. Muller JM, Isele U, Metzger E, Rempel A, Moser M, Pscherer A *et al*. FHL2, a novel tissue-specific coactivator of the androgen receptor. *EMBO J* 2000;**19**:359–369.
25. Vlahopoulos S, Zimmer WE, Jenster G, Belaguli NS, Balk SP, Brinkmann AO *et al*. Recruitment of the androgen receptor via serum response factor facilitates expression of a myogenic gene. *J Biol Chem* 2005;**280**:7786–7792.
26. Chan KK, Tsui SK, Lee SM, Luk SC, Liew CC, Fung KP *et al*. Molecular cloning and characterization of FHL2, a novel LIM domain protein preferentially expressed in human heart. *Gene* 1998;**210**:345–350.
27. Adams KF Jr, Dunlap SH, Sueta CA, Clarke SW, Patterson JH, Blauwet MB *et al*. Relation between gender, etiology and survival in patients with symptomatic heart failure. *J Am Coll Cardiol* 1996;**28**:1781–1788.
28. O'Meara E, Clayton T, McEntegart MB, McMurray JJ, Pina IL, Granger CB *et al*. Sex differences in clinical characteristics and prognosis in a broad spectrum of patients with heart failure: results of the Candesartan in Heart failure: Assessment of Reduction in Mortality and morbidity (CHARM) program. *Circulation* 2007;**115**:3111–3120.
29. Lindenfeld J, Ghali JK, Krause-Steinrauf HJ, Khan S, Adams K, Goldman S *et al*. Hormone replacement therapy is associated with improved survival in women with advanced heart failure. *J Am Coll Cardiol* 2003;**42**:1238–1245.
30. Gao XM, Agrotis A, Autelitano DJ, Percy E, Woodcock EA, Jennings GL *et al*. Sex hormones and cardiomyopathic phenotype induced by cardiac beta 2-adrenergic receptor overexpression. *Endocrinology* 2003;**144**:4097–4105.
31. Toma M, McAlister FA, Coglianese EE, Vidi V, Vasaiwala S, Bakal JA *et al*. Testosterone supplementation in heart failure: a meta-analysis. *Circ Heart Fail* 2012;**5**:315–321.